

JOINT INSTITUTE FOR NUCLEAR RESEARCH

**Proposal for Extension**  
**Participation of JINR in the NA61/SHINE**  
**experiment at the CERN SPS**  
**(theme 02-1-1087-2009/2020)**

**Annotation**

**Spokesperson from CERN:**

Marek Gazdzicki (marek.gazdzicki@cern.ch)

**Leader from JINR:**

Alexander Malakhov (malakhov@lhe.jinr.ru)

**Deputy leader from JINR:**

Georgy Melkumov (melk@mail.cern.ch)

**Participants:**

V.A. Matveev (*JINR management*);

D.A. Artemenkov, V.A. Babkin, M.G. Buryakov,  
V.M. Golovatyuk, D.K. Dryablov, V.A. Kireyeu, V.I. Kolesnikov,  
A.I. Malakhov, G.L. Melkumov, M.M. Romyantsev, R. Tsenov  
(*Veksler and Baldin Laboratory of High Energy Physics, JINR*);

S.A. Bunyatov, A.V. Krasnoperov, G.I. Lykasov, V.V. Lyubushkin, B.A.  
Popov, V.V. Tereshchenko (*Dzelepov Laboratory of Nuclear  
Problems, JINR*);

B. Baatar (*Institute physics and Technology of Mongolian  
Academy of Science, Ulaanbaatar, Mongolia*);

D. Kolev, M. Bogomilov (*Sofia University "St. Kliment Ohridski", Bulgaria*)

2017

## Participating Institutions

University of Athens, Athens, Greece  
University of Belgrade, Belgrade, Serbia  
University of Bergen, Bergen, Norway  
University of Bern, Bern, Switzerland  
Wigner Research Centre for Physics of the Hungarian Academy of Sciences, Budapest, Hungary  
Cape Town University, Cape Town, South Africa  
Jagellonian University, Cracow, Poland  
Joint Institute for Nuclear Research, Russia  
Fachhochschule Frankfurt, Frankfurt, Germany  
University of Frankfurt, Frankfurt, Germany  
University of Geneva, Geneva, Switzerland  
University of California, Irvine, USA  
Forschungszentrum Karlsruhe, Karlsruhe, Germany  
University of Silesia, Katowice, Poland  
Świetokrzyska Academy, Kielce, Poland  
Institute for Nuclear Research, Moscow, Russia  
LPNHE, University of Paris VI and VII, Paris, France  
Pusan National University, Pusan, Republic of Korea  
St. Petersburg State University, St. Petersburg, Russia  
State University of New York, Stony Brook, USA  
R. Idczaki, N. Katrynska, L. Turko  
Soltan Institute for Nuclear Studies, Warsaw, Poland  
Rudjer Boskovic Institute, Zagreb, Croatia  
ETH, Zurich, Switzerland

This document presents an abstract of the proposal for an extension of JINR participation in the full scientific programme of the NA61/SHINE experiment (SPS Heavy Ion and Neutrino Experiment) aimed in study of hadro-production in hadron-nucleus interactions and nucleus-nucleus collisions at the CERN SPS.

## **Contents**

Introduction	4
Physics research program of NA61/SHINE	6
Experimental apparatus	11
Recent results of NA61/SHINE	13
Status of the data taking and plans for 2018-2020	19
Contributions of the JINR group and working plans for 2018-20	20
Required resources	21

# 1. Introduction

One of the important issues of modern physics is the understanding of strong interactions and in particular the study of the properties of strongly interacting matter under extreme conditions. What are the phases of this matter and what do the transitions between them look like? These questions motivate broad experimental and theoretical efforts since more than 40 years. The study of high energy collisions between two atomic nuclei give us the unique possibility to address these issues in well controlled laboratory experiments. In particular, the theory of strong interactions, quantum chromodynamics (QCD), naturally led to expectations that matter at very high densities may exist in a state of quasi-free quarks and gluons, the quark-gluon plasma (QGP). A key problem was the identification of experimental signatures of QGP creation. Several such signatures of the formation of a transient QGP state during the early stage of the collision had been proposed: enhanced strangeness production and suppression of the open charm. Recent results on the energy dependence of hadron production in central Pb+Pb collisions at 20-158A GeV coming from the energy scan program at the CERN SPS [1] serve as evidence for the existence of a transition to the QGP state. The key results (Fig. 1): energy dependence of the mean pion multiplicity per wounded nucleon, of the  $(K^+)/(\pi^+)$  ratio and of the inverse slope parameter T of the transverse mass spectra of  $K^+$  mesons measured in central Pb+Pb (Au+Au) collisions.

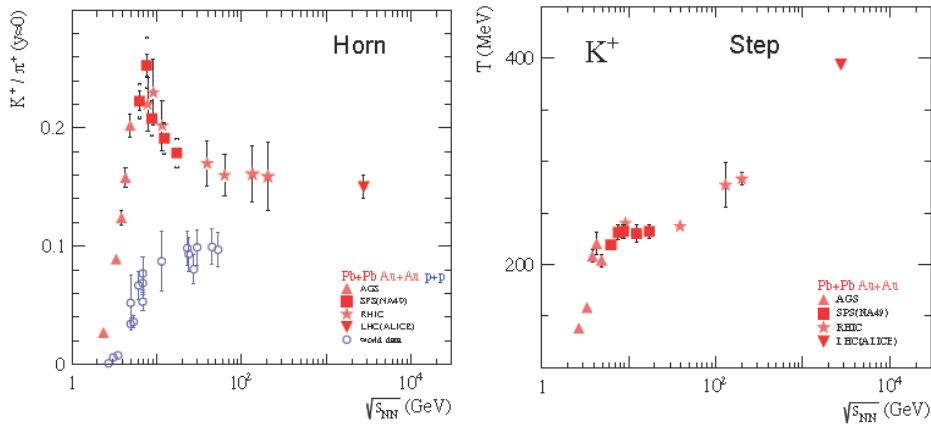


Figure 1: Energy dependence of  $K^+/p^+$  ratio (“Horn”) and slope parameter for kaons (“Step”) in central A+A and p+p interactions.

The stationary value of the apparent temperature of  $K^+$  mesons was predicted as a consequence of the constant pressure and temperature at the early stage of nucleus–nucleus collisions in the SPS energy range due to the coexistence of hadronic and deconfined phases. These properties of hadron production cannot be described satisfactory in the framework of traditional dynamical string-hadronic models which include re-scattering but not consider a phase transition.

The NA61 experiment was approved at CERN in June 2007 [2-8] and the proposed physics program consists of three main subjects:

- 1) Study of nucleus-nucleus collisions with the aim to identify the properties of the onset of deconfinement and find evidence for the critical point of strongly interacting matter.
- 2) Study of proton-proton and proton-nucleus interactions needed as reference data for better understanding of nucleus-nucleus reactions.

3) Measurements of hadron production in hadron-nucleus interactions needed for neutrino (T2K) and cosmic-ray experiments (Pierre Auger Observatory and KASCADE).

The nucleus-nucleus program has the potential for an important discovery – the experimental observation of the critical point of strongly interacting matter. We intend to carry out for the first time in the history of heavy ion collisions a comprehensive scan in two dimensional parameter space: size of colliding nuclei versus interaction energy. Other proposed studies belong to the class of precision measurements. The collaboration proposes to perform these measurements using the upgraded NA49 apparatus [9]. The most essential upgrades are an increase of data taking and event rate by an order of magnitude and the construction of a projectile spectator detector which will improve the accuracy of determination of the number of projectile spectators by a factor of about 20. The main advantage of NA61 experiment is large experimental acceptance (>60% of the full phase-space), as well as high tracking and PID capability. Synergy of different physics programs as well as the use of the existing detector set up and beam line offer the unique opportunity to reach the ambitious physics goals in a very efficient and cost effective way.

In the field of heavy-ion collision studies there is only one competing experiment which is running now – the STAR experiments at RHIC (BNL). It is a collider experiment which is able to cover the midrapidity region only. Moreover, in the region of collision energies  $\sqrt{s} < 7$  GeV the STAR event rate drops down to large extent since the RHIC luminosity decreases by lowering the beam energy. New experimental setups: NICA/MPD and CBM/FAIR will start to take data only in the next decade. So, the NA61/SHINE experiment at CERN/SPS (together with the STAR at RHIC) are the only experiments that are providing new precise experimental data in the energy range from 5 to 20A GeV. A report from the Villars meeting on "Fixed-Target Physics at CERN beyond 2005" [10] recognizes that the ion beams at the CERN SPS remain ideal tools to study the features of the phase transition between confined and deconfined states of strongly interacting matter. It notes that an ion program aimed at the identification of the critical point and the study of its properties is likely to be of substantial significance. The NA61 goals to measure hadron production in hadron-nucleus interactions needed for neutrino and cosmic-ray experiments as well as a search for the critical point in nucleus-nucleus collisions were summarized in the Briefing Book for European Strategy for Particle Physics [11].

JINR physicists actively participate in the NA61/SHINE experiment from the very beginning. The main fields of activity of the JINR group are the Time-Of-Flight detector maintenance, software development, data taking, and analysis.

This document is organized as follows. The physics program of the NA61 experiment is discussed in Section 2. The existing NA61 detector and the required upgrades are described in Section 3. In Section 4 the recent physics results are presented. The status of the data taking is presented in Section 5, the JINR contribution, a working plan of the JINR group for the period 2018-20, and requested resources are presented in Section 6.

## 2. Physics Research Program of NA61/SHINE

### 2.1 Study of the properties of the deconfinement phase transition

As it was mentioned in the Introduction, non-monotonic energy dependence in hadron production from central Pb+Pb collisions (NA49 ‘‘Horn’’ and ‘‘Step’’) serve as evidence for the onset of deconfinement phase transition at low SPS energies. Further progress in understanding effects which are likely related to the onset of deconfinement can be done only by a new comprehensive study of hadron production in proton-nucleus and nucleus-nucleus collisions. The two most important open questions are:

- what is the nature of the transition from the anomalous energy dependence measured in central Pb+Pb collisions at SPS energies to the smooth dependence measured in p+p interactions?
- is it possible to observe the predicted signals of the onset of deconfinement in event-by-event fluctuations?

In order to achieve the qualitative progress in the experimental situation the NA61 experiment proposed to perform new detailed energy scan in reactions from elementary p+p to Pb+Pb collisions at several collision energies, namely, data taking at 13A, 20A, 30A, 40A, 80A, and 158A GeV/c. Within a data-taking period (2014-2017) data at all energies can be recorded with a typical event statistics of about 10 times the one of the NA49 data. This, together with the important detector upgrades, will allow to significantly decrease statistical and systematic uncertainties of results on Pb+Pb collisions by superseding the NA49 results with new NA61/SHINE measurements. This in turn will allow to reach significantly higher precision in establishing the system size dependence of hadron production properties, which is relevant for the onset of deconfinement, as it is illustrated in Fig. 2 using as an example the  $K^+/\pi^+$  ratio.

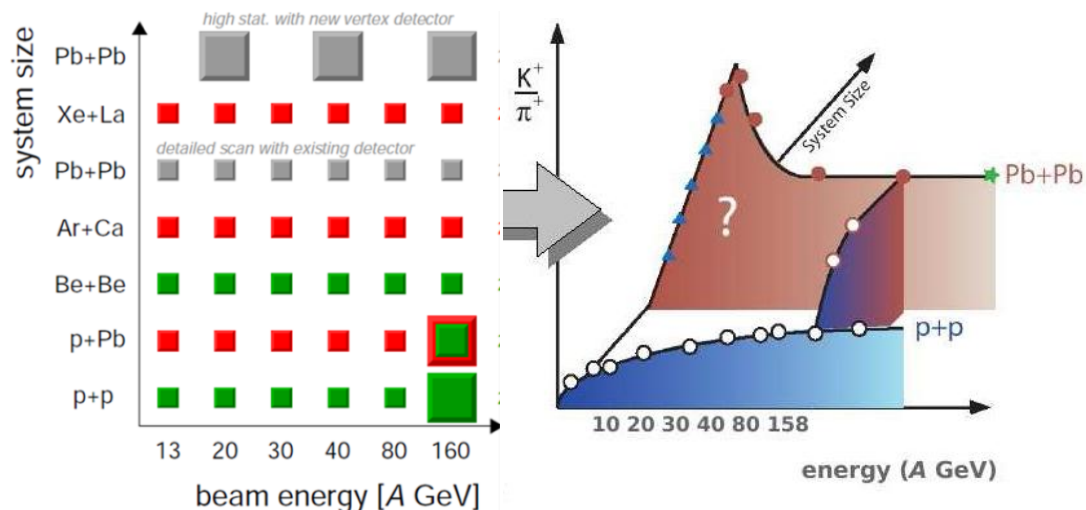


Figure 2: An illustration of the impact of the new measurements on clarifying the system size dependence of the  $K^+/\pi^+$  anomaly observed in central Pb+Pb collisions at the low SPS energies.

The performance of the fully upgraded NA61 experiment with respect to physics of nucleus-nucleus collisions will be qualitatively improved in comparison to the

performance of NA49. The increase of data taking and event rate by a factor of more than 20 will allow for a comprehensive two-dimensional scan in collision energy and mass of the colliding nuclei.

## 2.2 Critical point

Fig. 3 shows a sketch of the phases of strongly interacting matter in the  $(T, \mu_B)$  plane as suggested by QCD-based considerations. To a large extent these predictions are qualitative, as QCD phenomenology at finite temperature and baryon number is one of the least explored domains of the theory. Lattice QCD-based calculations suggest a rapid crossover from the hadron gas to the QGP at the temperature  $T_C = 170 - 190$  MeV and the nature of the transition to QGP is expected to change with increasing baryochemical potential. At high potential the transition may be of the first order, with the end point of the first order transition domain (marked E in Fig. 3, left), being the critical point of the second order. The position of the critical region is uncertain, but the best theoretical estimates based on lattice QCD calculations locate it at  $T \sim 158$  MeV and  $\mu_B \sim 360$  MeV [12, 13] as indicated in Fig. 3. A characteristic property of the second order phase transition (the critical point or line) is a divergence of the susceptibilities. Consequently an important signal of a second-order phase transition at the critical point are large fluctuations, in particular an enhancement of fluctuations of multiplicity and transverse momentum are predicted [14].

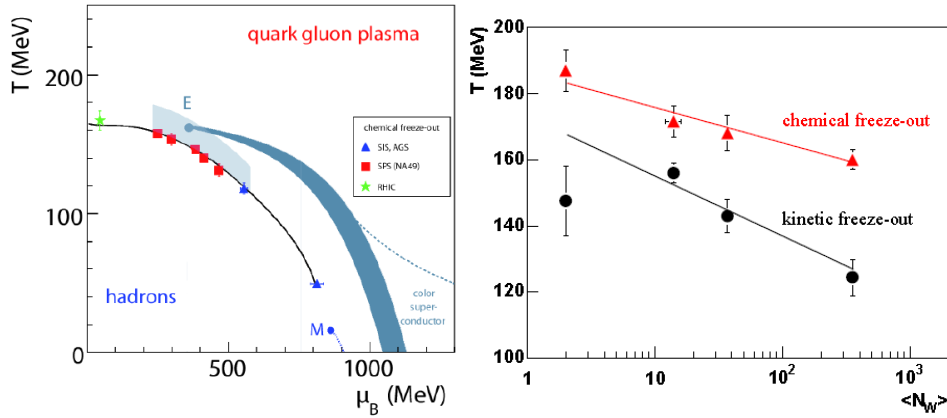


Figure 3: (Left) The QCD phase diagram in terms of temperature ( $T$ ) and baryo-chemical potential ( $\mu_B$ ). E marks the end point E of the first order transition line and the region covered by the future measurements at the CERN SPS is indicated by the gray band. (Right) The dependence of the chemical and kinetic freeze-out temperatures on the mean number of wounded nucleons for p+p, C+C, Si+Si and Pb+Pb collisions at 158A GeV.

Employing such techniques in a study of nuclear collisions at different energies at the SPS and with nuclei of different sizes, the experiment may test not only the existence and location of the critical point but also the size of critical fluctuations as given by the critical exponents of the QCD conjecture. Thus when scanning the phase diagram a maximum of fluctuations located in a domain close to the critical point (the increase of fluctuations can be expected over a region  $T \sim 15$  MeV and  $\mu_B \sim 50$  MeV) or the critical line should signal the second order phase transition. It is thus in the vicinity of the chemical freeze-out points of central Pb+Pb collisions at the CERN SPS energies. Pilot data [15] on interactions of light nuclei (Si+Si, C+C and p+p) taken by NA49 at 40A and 158A GeV indicate that the freeze-out temperature increases with decreasing mass number,  $A$ , of the colliding nuclei (see Fig. 3, right). This means that a scan in the collision energy and mass of the colliding nuclei allows us to scan the  $(T, \mu_B)$  plane in a search for the critical point (line) of strongly interacting matter [16]. The experimental search for the critical point by investigating nuclear collisions is justified at energies higher than

the energy of the onset of deconfinement. This is because the energy density at the early stage of the collision, which is required for the onset of deconfinement is higher than the energy density at freeze-out, which is relevant for the search for the critical point. The physics goals of the new experimental program with nuclear beams at the CERN SPS presented in the previous section require a comprehensive energy scan in the whole SPS energy range (10A-158A GeV) with light and intermediate mass nuclei. The NA61 collaboration intends to register p+p, Be+Be, Ar+Ar and Xe+Xe collisions at 13A, 20A, 30A, 40A, 80A, 158A GeV and a typical number of recorded events per reaction and energy of 6 MEvents.

### 2.3 Reference p+p, p+A data

An interpretation of the experimental results on nucleus-nucleus collisions at high energies relies to a large extent on a comparison with the corresponding data on p+p and p+A interactions. However, the available p+p and p+A results concern mainly basic properties of hadron production and they are sparse. Thus large statistic of such interaction would be desirable, and by the time they were not systematically measured. One of the most striking features observed at BNL-RHIC is the suppression of high pT hadron production in central A+A collisions relative to peripheral A+A collisions (“jet quenching”). This is generally interpreted as a sign of parton energy loss in hot and dense hadronic matter created at the early stage of nucleus-nucleus collisions. This interpretation implies that the suppression should disappear at low energies where the energy density is not enough for creation of the deconfined state of matter. Thus it is crucial to extend the study of the energy dependence to high-pT production, in particular in the CERN SPS energy range.

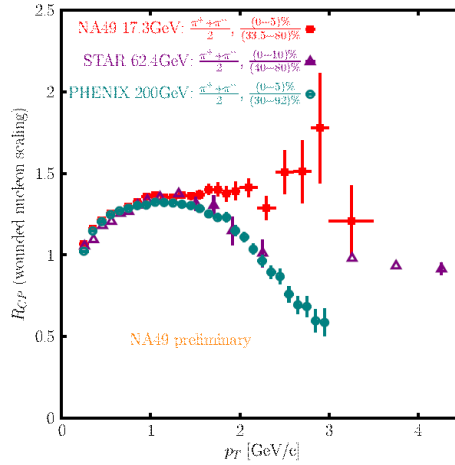


Figure 4: The ratio ( $R_{CP}$ ) of pion transverse momentum spectra of central to peripheral Pb+Pb interactions at 158A GeV as measured by NA49 [17].

The NA49 and other CERN SPS experiments measured identified hadron production in Pb+Pb collisions at 158A GeV up  $p_t \sim 3-4$  GeV/c [18]. The first results expressed in terms of the ratio of the pT-spectra measured in central and peripheral collisions ( $R_{CP}$ ) are shown in Fig. 4 where the corresponding results at RHIC energies are also plotted for comparison. The suppression seems to weaken gradually with decreasing collision energy. The key measure in this study is, however, the ratio between pT spectra measured in central Pb+Pb collisions and p+p interactions,  $R_{AA}$ . Thus precision p+p data are crucial for an interpretation of the A+A results. The statistics of the NA49 p+p published data ( $3 \cdot 10^6$  events) at 158 GeV, however, ends at about  $p_t = 2.6$  GeV/c. All this leads to a large systematic uncertainty of the estimate of the high  $p_t$  tail of the p+p spectrum based on an extrapolation of the existing data and a need for high statistics and high precision measurements of identified hadron production in p+p and p+A collisions at SPS energies is indeed very urgent. An increase of event statistics by a factor of

above 10 would extend the  $p_t$  coverage to about 4 GeV/c. Moreover, many needed data on fluctuations, correlations and, in particular, on particle production at high transverse momenta are missing. Thus, new measurements of hadron production in p+p and p+A reactions are necessary and should be performed by NA61 in parallel to the corresponding measurements for A+A collisions. The additional advantage of data recorded by NA61/SHINE will be that all the interactions, together with nucleus-nucleus measured by NA49 experiment, are recorded by the same detector.

## 2.4 Measurements for Fermilab neutrino beams.

NA61/SHINE has recently started on a program of hadron production measurements to benefit the Fermilab neutrino program. The current NuMI beam uses 120 GeV/c protons on a graphite target to produce neutrinos, and serves the MINOS+, Minerva, and NOvA experiments. The proposed future LBNF beamline from Fermilab to South Dakota will provide an even higher intensity beam using protons with an energy between 60-120 GeV/c (still to be determined) on a graphite or possibly beryllium target. In addition to measurements of the particles produced by the interactions of the primary beam protons, the hadrons produced by secondary interactions of lower-energy protons and pions in the target and aluminum horns also contribute significantly to the neutrino flux. NA61/SHINE is well-suited to make measurements that can reduce the flux uncertainties for the Fermilab neutrino experiments.

## 2.5 Experimental landscape related to the NA61 ion program.

The exciting and rich physics topics which can be studied in nucleus-nucleus collisions at the CERN SPS energies also motivates physicists from BNL, JINR and FAIR to perform experimental studies in this energy range which will complement the CERN SPS program. Figure 5 shows a world map indicating laboratories and experiments which plan to carry out measurements of nucleus-nucleus collisions at CERN SPS energies within the next 10 years. Two fixed target programs (CERN SPS and FAIR SIS-300 [19]) and two programs with ion colliders (BNL RHIC [20] and JINR NICA [21]) are foreseen. The SPS and RHIC energy range covers energies significantly below and significantly above the energy of the onset of deconfinement ( $\approx 30A$  GeV in the fixed target mode). Thus these machines are well suited for the study of the properties of the onset of deconfinement and the search for the critical point. The top energies of NICA and SIS-300 are just above the energy of the onset of deconfinement. The physics at these machines thus focuses on the study of measurements of nucleus-nucleus collisions at CERN SPS energies within the next 10 years properties of dense confined matter close to the transition to the QGP.

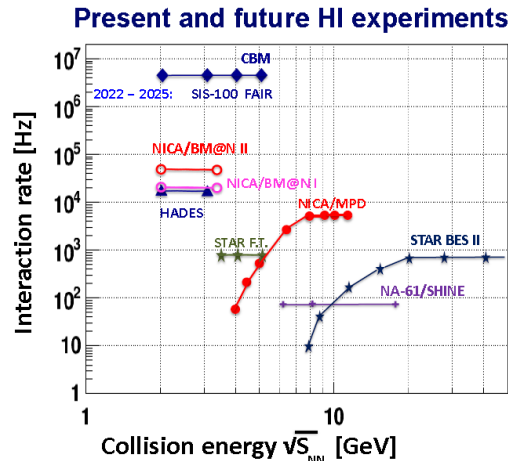


Figure 5: The main parameters of the experimental programs studying nucleus-nucleus collisions within the next 10 years.

The advantages of the NA61 ion program over the RHIC energy scan program are:

- measurements of identified hadron spectra in a broad rapidity range which allow to obtain the mean hadron multiplicities in full phase-space,
- measurements of the total number of the projectile spectator nucleons comprising free nucleons and nucleons bound in nuclear fragments,
- high and similar event rate over the full SPS energy range including the lowest energies,
- high flexibility in selecting the nuclear mass number (thanks to the secondary ion beam) and energy (thanks to the SPS features) of the projectile ions

### 3 Experimental apparatus

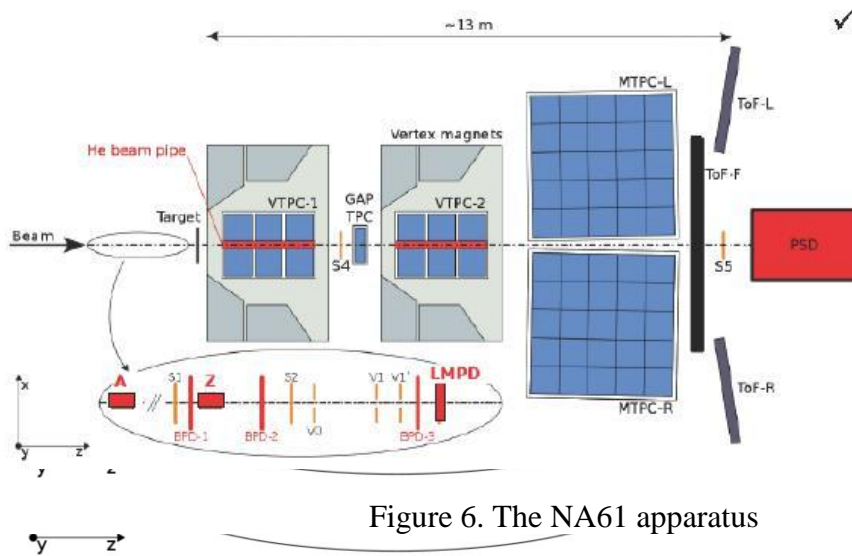


Figure 6. The NA61 apparatus

The NA61 experiment (Fig.6) was a large acceptance hadron spectrometer at the CERN-SPS for the study of the hadronic final states produced in various reactions (from p+p to Pb+Pb). The main tracking devices were four large volume Time Projection Chambers (TPCs), which are capable of detecting 70% of the approximately 1500 charged particles created in a central Pb+Pb collision at 158A GeV. Two of them, the vertex TPCs (VTPC-1 and VTPC-2), are inside the magnetic field of two super-conducting dipole magnets (1.5 and 1.1 T, respectively) and two others (MTPC-L and MTPC-R) are positioned downstream of the magnets. The NA61 TPCs allowed precise measurements of particle momenta  $p$  with a resolution of  $\sigma(p)/p^2 \approx (0.3 - 7) \cdot 10^{-4} (\text{GeV}/c)^{-1}$ . The set-up was supplemented by two time of flight detector arrays (TOF-F, TOF-L and TOF-R) detector arrays with a time measurement resolution from 60 to 100 ps and a Projectile Spectator Detector (PSD). The positions of the incoming beam particles in the transverse plane are measured by a telescope of three Beam Position Detectors (BPD1-3) placed along the beam line upstream of the target. The beam-line set of detectors consists of the S1 counter (0.5 cm thick scintillator equipped with four photomultipliers), the second beam counter S2 (0.2 cm thick located just behind the BPD-2), two 1 cm thick veto scintillator detectors (V0,1), and S4 and S5 detectors (2 cm diameter, 0.5 cm thickness located downstream of the target). The time-of-flight TOF-L/R detector, the JINR group is responsible for, consists of 1800 scintillator pixels read out with FEU-87 (TOF-L) and Hamamatsu R1828 (TOF-R) photomultipliers. The size of each scintillator pixel is  $7 \times 3,4 \times 2.5$  cm. The time resolution of the TOF-L/R walls of 60 ps provides a  $5\sigma \pi/K$  separation at 3 GeV/c.

The most important facility modifications performed during the 2015-17 are briefly summarized below:

- Installation of a new Magnet Safety System (MSS) to replace the old protection in VERTEX-1 and VERTEX-2 system was complete in 2016. The cryogenic system was maintained, repaired, and its parameters were optimized.
- An additional short PSD module of 1.2 nuclear interaction length and transverse dimension of  $10 \times 10$  cm<sup>2</sup> was constructed and installed in order to fix the problem of escaping of a part of hadronic shower through the rear side of the calorimeter. Also, the readout MAPD-3A photodiodes in central modules were replaced by fast silicon photo-

multipliers MPPCs S12572-010C/P recently developed by Hamamatsu Co, and the cooling system for MAPDs was upgraded to one based on a vortex tube.

### Software and Calibration procedure.

The new software framework for NA61, called SHINE is written in C++ and designed to comprise three principal parts: a collection of processing modules which can be assembled and sequenced by the user via XML files, an event data model which contains all simulation and reconstruction information based on STL and ROOT streaming, and a detector description which provides data on the configuration and state of experiment. Currently the NA61/SHINE uses the new framework SHINE for data analysis and quality assessments. The native SHINE Monte Carlo simulation consists of major two steps; a GEANT 4 based detector description to simulate the passage of particles through detectors and a digitization simulation to simulate the detector responses. A GEANT 4 based detector description in SHINE (Luminance) is fully implemented including all the NA61 sub-systems. The Luminance outputs are then fed into the digitization process which simulates the detector response and outputs raw detector simulated signals. The old (“legacy”) code calculating the drift of charge clouds in the TPCs has been re-written in SHINE with improved maintainability and precision. Validations toward the data have been done (see an example in Fig. 7).

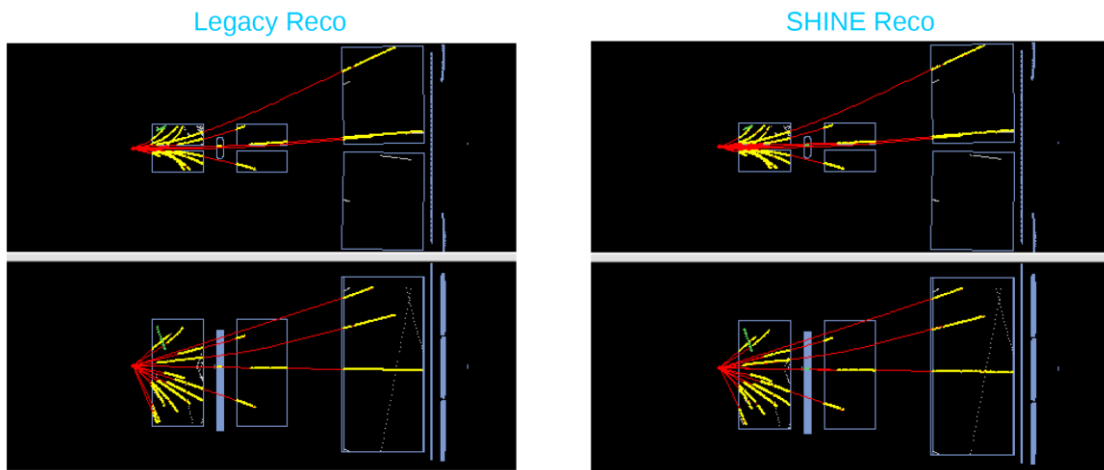


Fig. 7 A comparison using a same p+C event with “legacy” MC simulation (left) and SHINE MC simulation (right).

## 4. Recent results of NA61/SHINE

The very recent results of the NA61 experiment are published in [22-26]. Among them, the most interesting results to which the JINR group contributes are briefly summarized below. In addition to data taking and analysis, the JINR group has performed several tests of new mRPC-based prototypes for the planned upgrade of the NA61 TOF-L/ detector.

1. **“Measurements of  $\pi^{+/-}$ ,  $K^{+/-}$ ,  $K_s^0$ ,  $\Lambda$  and proton production in proton-carbon interactions at 31 GeV/c with the NA61/SHINE spectrometer at the CERN SPS”**  
**Eur. Phys. J. C (2016) 76:8**

Measurements of hadron production in p + C interactions at 31 GeV/c were performed using the NA61/SHINE spectrometer at the CERN SPS. Final results have been recently published in [22]. Inelastic and production cross sections as well as spectra of  $\pi$ , K, p,  $K_s^0$  and  $\Lambda$  have been measured with a high precision. The analysis is based on  $3 \cdot 10^6$  events from a graphite target with a thickness of 4 % of a nuclear interaction length. The data analysis procedure consists of the following steps: application of event and track selection criteria, determination of spectra of hadrons using the selected events and tracks, evaluation of corrections to the spectra based on experimental data and simulations, calculation of the corrected spectra. Corrections for the following biases were evaluated and applied: geometrical acceptance, reconstruction efficiency, contribution of off-target interactions, contribution of other (misidentified) particles, feed-down from decays of neutral strange particles, analysis-specific effects (e.g. ToF efficiency, PID,  $K^-$  contamination, etc.).

The combined tof -dE/dx analysis technique was employed to determine yields of  $\pi^\pm$ ,  $K^\pm$  and protons in the momentum region above 1 GeV/c. For lower momenta measurements of the specific energy loss dE/dx of charged particles by ionization in the TPC gas are used for their identification.  $\Lambda$ -hyperons and  $K_s^0$  are identified by reconstructing their decay topology. Pairs were formed from all measured positively and negatively charged particles. V0 candidates were required to have a distance of closest approach between the two trajectories of less than 1 cm anywhere between the position of the first measured points on the tracks and the primary vertex. In the second step, the position of the secondary vertex and the momenta of the decay tracks were fitted by performing a 9-parameter  $\chi^2$  fit employing the Levenberg–Marquardt fitting procedure. The selected V0 candidates are binned in {p,  $\theta$ } phase space. Due to detector acceptance and reconstruction efficiency, the momentum range of reconstructed charged particles starts from 0.4 GeV/c. For the KOS analysis, 28 bins are used, whereas the  $\Lambda$  candidates are divided into 39 bins. The choice of the binning scheme is driven by the available statistics

The raw yield was obtained by performing a fit of the invariant mass spectra with the sum of a background and a signal function. The shape of the signal was described by the Lorentzian function, the background was represented by a Chebyshev polynomial of 2<sup>nd</sup> order. The uncertainty introduced by choosing this particular functional form was estimated by trying other background functions. The results for  $K^+$  and  $K_s^0$  measured with high precision are shown in Fig. 8 and 9, respectively. These measurements are essential for improved calculations of the initial neutrino fluxes in the T2K long-baseline neutrino oscillation experiment in Japan. A comparison of the NA61/SHINE measurements with the predictions of several hadroproduction models are also presented.

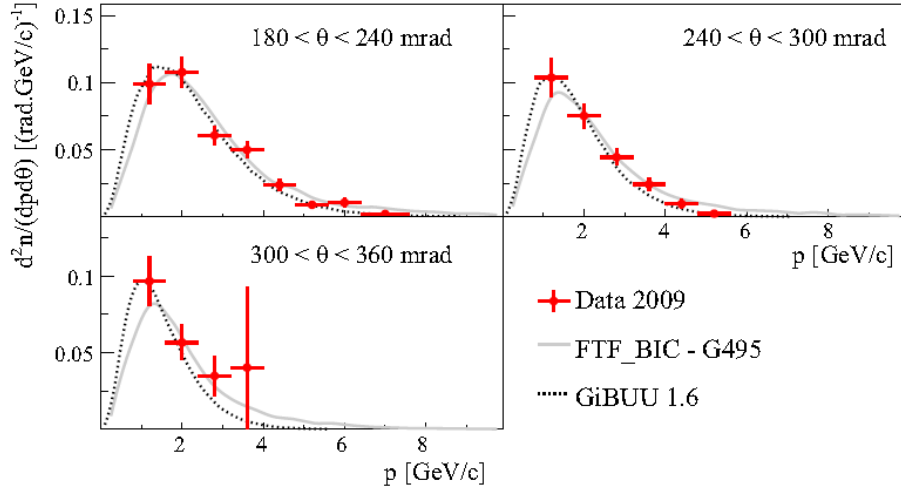


Fig. 8. Laboratory momentum distributions of  $K^+$  mesons produced in p+C interactions at 31 GeV/c in different polar angle intervals. Distributions are normalized to the mean  $K^+$  multiplicity in all production p+C interactions. Vertical bars show the statistical and systematic uncertainties added in quadrature, horizontal bars indicate the size of the momentum bin. The overall uncertainty due to the normalization procedure is not shown. The spectra are compared to predictions of the FTF\_BIC-G495 and GiBUU1.6 models.

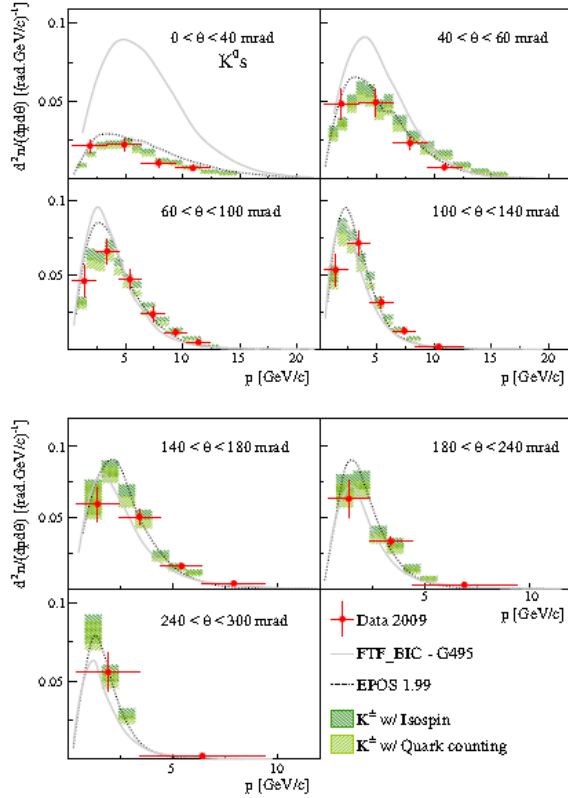


Fig. 9. Laboratory momentum distributions of  $K_S^0$  mesons produced in p+C interactions at 31 GeV/c in different polar angle intervals. Distributions are normalized to the mean  $K_S^0$  multiplicity in all production p+C interactions. Vertical bars show the statistical and systematic uncertainties added in quadrature, horizontal bars indicate the size of the momentum bin. Shaded boxes show predictions obtained from  $K^+$  yields using isospin (dark green) and quark counting (light green) hypotheses. The spectra are compared to predictions of the FTF\_BIC-G495 and Epos1.99 models.

These measurements are essential for predictions of the initial neutrino and antineutrino fluxes in the T2K long baseline neutrino oscillation experiment in Japan. They have already been used for the updated T2K results presented during 2016 summer conferences. Furthermore, these measurements provide important input to improve hadron production models needed for the interpretation of air showers initiated by ultrahigh energy cosmic particles.

## 2. "Production of deuterium, tritium, and $^3\text{He}$ in central Pb+Pb collisions at 20A, 30A, 40A, 80A, and 158A GeV at the CERN SPS" Phys. Rev. C 94 044906 (2016).

In [26] production of deuterons, tritons, and helium-3 nuclei in central Pb+Pb interactions was studied at five center-of-mass collision energies from 6 to 17 GeV per nucleon. The identification of light nuclei was based on momentum,  $dE/dx$ , and time-of-flight measurements. Deuteron candidates were required to have a TOF hit matched to the MTPC track, while the identification of  $^3\text{He}$  candidates can rely completely on the specific energy loss measurement in the MTPC gas. The raw yields of clusters were corrected for geometrical acceptance, detector efficiency, and for the losses due to the PID selection criteria. The corrections were obtained from Monte Carlo (MC) simulations and from the data itself. The invariant  $m_t$ -spectra of identified  $^3\text{He}$  nuclei at five collision energies in different rapidity intervals are shown in Fig. 10. The NA49 acceptance for light nuclei is sufficient to examine spectra in several rapidity intervals and their sizes are indicated in the figure. The experimental distributions are scaled down successively for clarity.

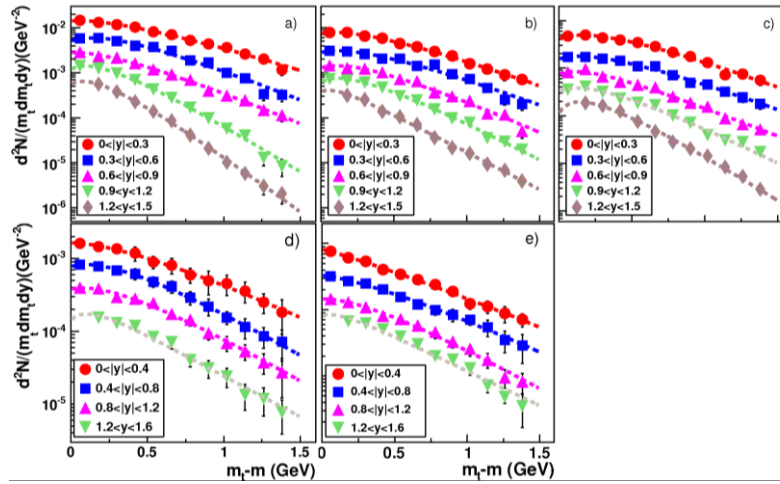


Fig. 10. Invariant  $m_t$ -spectra of  $^3\text{He}$  at 20A (a), 30A (b), 40A (c), 80A (d), and 158A GeV (e). Only statistical errors are shown. The distributions near mid-rapidity are drawn to scale, other spectra are scaled down by successive powers of 5 for clarity.

In order to obtain particle rapidity density ( $dN/dy$ ) we summed the measured points over the distributions and added the extrapolations into unmeasured  $m_t$  regions exploiting information on the spectral shape. The overall systematic uncertainty for the yields of  $^3\text{He}$  is of about 6% at mid-rapidity and approximately 10% for the most forward rapidity bin. For deuterons the systematic uncertainty varies from 5% to 15% depending on rapidity interval. The cluster yields are plotted in Fig. 11 as a function of the normalized rapidity  $y/y_{\text{beam}}$ . All the rapidity distributions are concave and in order to quantify the shape all the data points were fitted with a parabola  $a+b (y/y_{\text{beam}})^2$  (the fits are shown by dashed lines). The ratio of the fit parameters  $b/a$  (relative concavity) tends to increase with increasing beam momentum and cluster mass. Such a behavior of the invariant yields versus rapidity was earlier observed at AGS energies [27], where the relative concavity of the yield of clusters with atomic mass number from  $A=2$  to 4 progressively increases with  $A$ .

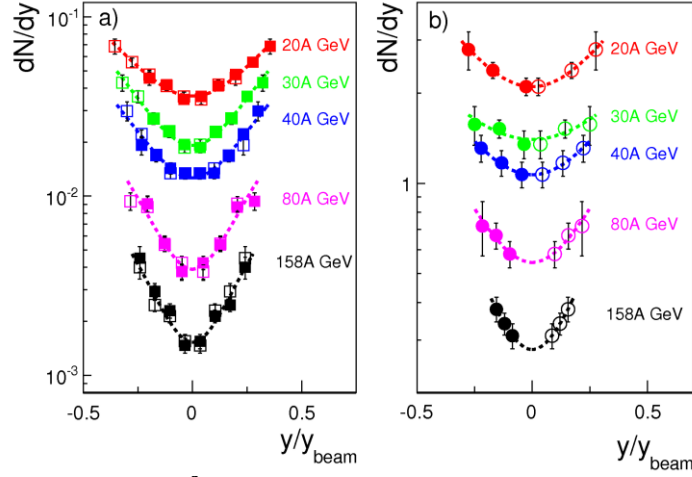


Fig. 11. Rapidity distributions for  ${}^3\text{He}$  (a) and deuterons (b) from central Pb+Pb collisions at 20A-158A GeV as a function of normalized rapidity  $y/y_{\text{beam}}$ . The solid symbols show the measurements and the open ones are the data points reflected around mid-rapidity. Dashed lines indicate parabolic fits to the rapidity spectra.

The total yield was then obtained by summing the measured values with the integral of the corresponding extrapolation function over the unmeasured region. To extrapolate the integral of  $dN/dy$  to full phase space, averaging of two different parameterizations of the rapidity spectra were employed as explained in Ref. [28]. The extrapolation accounts from 30% to 63% and from 20% to 85% of the total yield for  ${}^3\text{He}$  and d, respectively, depending on the collision energy. The estimates for the total yield of deuterium and helium nuclei are plotted in Fig. 12 with red squares.

In the framework of a statistical thermal model the abundance  $N_C$  of a nucleon cluster of mass  $m$ , degeneracy factor  $g$ , charge  $q$ , and baryon number  $B$  is given by

$$N_C = \frac{gV}{\pi^2} m^2 T K_2\left(\frac{m}{T}\right) \exp\left(\frac{B\mu_B + q\mu_q}{T}\right) \quad (4.1)$$

where  $V$ ,  $T$ ,  $m_B$ ,  $m_q$ , and  $K_2$  are the source volume, temperature, baryochemical potential, charge potential, and Bessel function of the second kind. Such models have been able to reproduce the multiplicities of different types of particles in elementary and heavy-ion interactions. There are several parameterizations for the thermal fireball parameters  $T$ ,  $m_B$ , and  $V$  (or equivalently the fireball radius  $R$ ) over a wide range of nuclear collision energies from AGS to LHC [29-32]. Using averages of these fireball parameters the mean multiplicities of d and  ${}^3\text{He}$  were computed at all five collision energies according to Eq. 4.1. The results are plotted in Fig. with blue circles. As it can be seen, thermal model calculations are capable of reproducing the energy dependence of the cluster multiplicities not only qualitatively but also quantitatively. The deviation of the calculations from the measured abundances does not exceed 2 standard deviations (see insets in Fig. 12). It appears at first glance that such a good agreement between experimental data on cluster production and thermodynamical model calculations looks surprising since one expects that chemical equilibrium of compound nucleon systems with the environment reaches later in time than the chemical freeze-out in the fireball has happened. The more diluted and colder matter is needed to make a net (fusion minus decomposition) rate positive for bound nucleon systems of several MeV binding energy. It has been recognized, however, that the light nuclei production process is basically determined by the entropy per baryon of the medium that is fixed at the chemical freeze-out [33]. During further isentropic expansion stage a dynamic equilibrium has been reached for the light nuclei population: the loss due to disintegration are balanced by the gain in newly produced clusters.

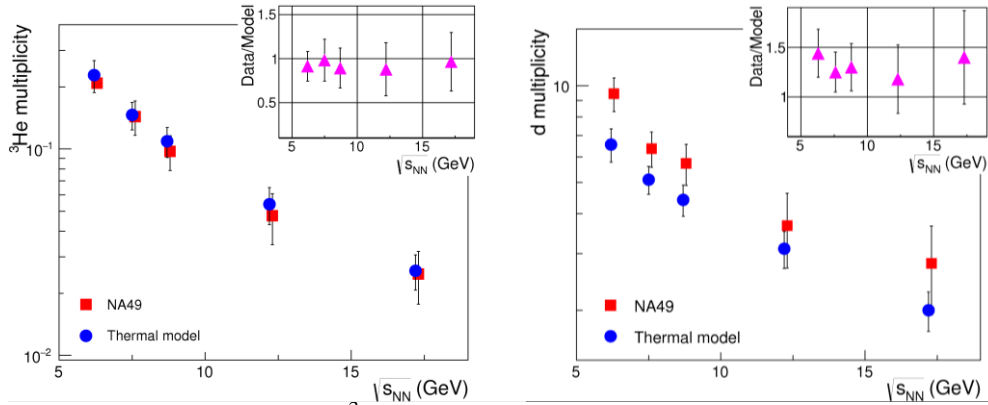


Fig. 12. The total yield of  ${}^3\text{He}$  (left panel) and deuterons (right panel) in central Pb+Pb collisions at 20A-158A~GeV. The NA49 data are shown by red squares, thermal model calculations are indicated by blue circles. The insets show the ratio of the experimental data to the thermal model predictions.

### 3. Beam tests of MRPC-based TOF detector prototypes.

At present, the time-of-flight (TOF) system for the NA61/SHINE heavy-ion program consists of the two walls of the 891-channel scintillation detectors constructed in 1995-96. This system, being 23 years old, requires an upgrade in order to be in operation for next several years, in particular, after 2020. The most critical part of the TOF system is the FASTBUS-based readout electronics with a very limited set of spare elements. A suggestion is to replace the TOF detector with a modern high-performance and cheap MRPC detector. Our Lab. has a solid background in construction and maintenance of such detectors.

A schematic drawing of the proposed MRPC module [34] is presented in Fig. 13. The detector consists of three stacks of 5 gas gaps each. Float glass was used as resistive electrodes. The outer glass electrodes have the thickness of 400  $\mu\text{m}$ . The internal glass electrodes have the thickness of 280  $\mu\text{m}$ . The fishing line as a spacer defines the 200  $\mu\text{m}$  gap between the all resistive electrodes. The outer part of external glass electrodes is covered by the conductive paint with surface resistivity about 10  $\text{M}\Omega/\square$  to apply high voltage. All internal glasses are floating. Overall dimensions of the detector ( $600 \times 300 \text{ mm}^2$ ) are determined by the size of the glass. 48 pickup electrodes with pitch of 12.5 mm look like strips and made at the inner layer of the PCB. It is necessary for better electrical isolation of strips from high voltage layer. The differential analog signal is transferred from the PCB to the front-end electronics (FEE) board by doubled twisted pair cable. FEE based on the NINO ASIC are designed by JINR [35]. The signal is read out from both ends of the strip. It provides better time resolution and determination of the coordinate of a particle along the strip. Digitizing of the signal is provided by the VME based time-to-digital converter TDC72VHL [36] designed by JINR. The native time resolution of the readout electronics is no more than 20 ps.

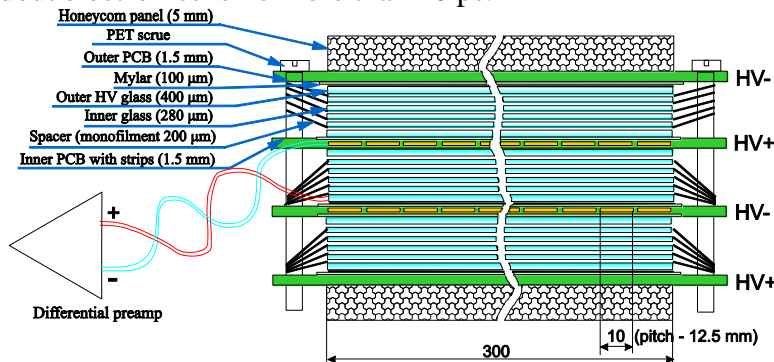


Fig. 13. Cut view of the triple-stack MRPC.

A prototype of the proposed MRPC was tested at CERN with the NA61 spectrometer in November 2016. Test setup was located just behind the existing TOF-L wall and registered secondary particles from the Pb-Pb interactions with beam energy of 30 GeV. The first test was performed using a stand-alone data acquisition system with two types of trigger. First type of the trigger was a coincidence of two scintillator counters located before and after MRPCs. Second type was the central interaction trigger (T2) of the NA61 DAQ. The system of two MRPCs with pad readout [37] was used as a reference to define the time resolution of the tested MRPC. The time resolution of the tested MRPC was estimated from the time distribution between tested MRPC and two “start” MRPCs (as demonstrated in Fig. 14). If one considers that the time resolution of the one pad MRPC is about 62 ps then can be asserted the time resolution of the system of two detectors is  $62/\sqrt{2} \cong 44$  ps. The time resolution of tested MRPC is  $\sqrt{66^2 - 44^2} \cong 50$  ps. The momentum spectrum of particles crossing the MRPCs are unknown, but we can ignore this fact because distance between tested MRPC and “start” MRPCs was small (of about 10 cm).

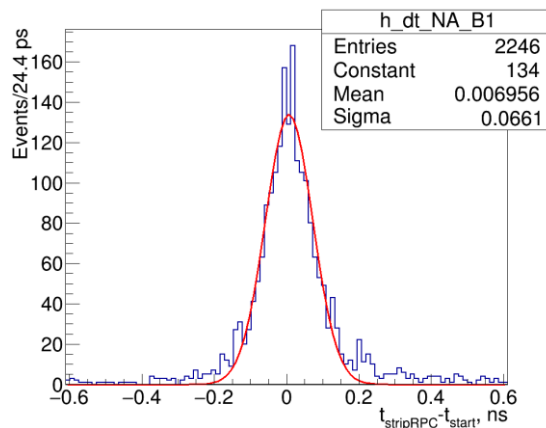


Fig. 14. Distribution of the time difference between tested MRPC and mean time of two reference MRPCs with pad readout

In Table 2 a rough estimate for the price of a MRPC-based TOF system for the case if NA61 decides to upgrade the detector is listed. If the area of the whole TOF is 4 m<sup>2</sup> (equal to the current TOF-L/R coverage) then it costs 308 k€. The cost of the gas system for the MRPC TOF is about 100 k€. Thus an estimate for the full price of the TOF system covering about 4 m<sup>2</sup> is ~400 €.

Table 2. Preliminary cost estimation of MRPC TOF system for NA61

Name of components	Price/ch, €	Price/1 m <sup>2</sup> (576 ch), €
FEE (NINO base)	12	6.9
TDC (HPTDC base)	32	18.4
Detectors (48 strips, 96 ch)	15	8.6
Crates, signal cables	52	30.0
LV, YV, cabling	16	9.2
Space frame, mechanical construction, gas box	7	4.0
Total	134 €/channel	77.1 k€/1 m <sup>2</sup>

Within the project it is planned to perform only R&D work on the MRPC system which costs 50 k€.

## 5. Status of the data taking and plans for 2018-2020.

The overall NA61 data taking scenario is shown in Figure 15, which schematically illustrates the status and plans for data-taking within the NA61/SHINE (beam momentum)-(system size) scan. The approved data-taking period for NA61/SHINE should be completed by the end of 2018.

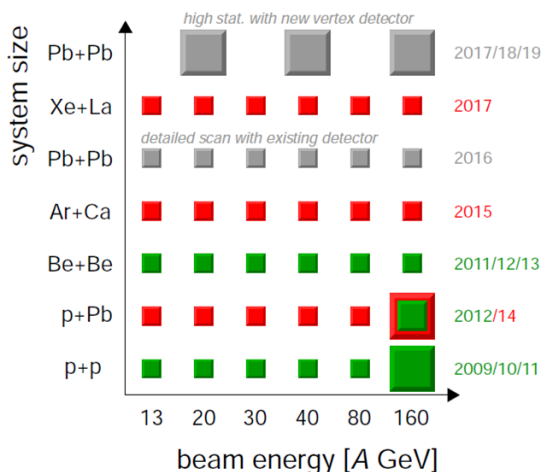


Figure 15: The NA61 data taking plan until 2019.

In November 2015 the Pb beam at 30 A GeV/c was used for detector tests for future heavy ion data taking and potential extension of the NA61/SHINE data taking program after Long Shutdown 2. The beam and beam line were successfully tested with  $10^6$  Pb ions/spill. It was verified that the TPCs operate correctly with high multiplicity Pb+Pb collisions. The test was necessary, because it was hypothesised that the gas amplification may become less stable due to removal of flammable methane from the gas mixture in NA61/SHINE.

The data taking period for Fermilab neutrino beams was started in September 2016, as scheduled. Table 3 lists the data already recorded within this program.

Table 3. Data collected in 2016.

beam	target	beam momentum	number of events
p	Pb	80 GeV/c	2.8M
p	C	60 GeV/c	2.8M
$\pi^+$	C	60 GeV/c	2.6M
p	C	120 GeV/c	4.1M
p	Al	60 GeV/c	3.2M
p	Be	60 GeV/c	3M*
$\pi^+$	Be	60 GeV/c	3M*
p	Be	120 GeV/c	3M*

The revised NA61/SHINE data-taking plans for 2017-18 is presented in Table 4. Following the current accelerator schedule the plan assumes that the data-taking with a primary Xe beam will take place in 2017 and with a Pb beam in 2018. It is also assumed that hadron beams will be available for several months in 2017 and 2018 until the Long Shutdown 2.

Table 4. The NA61/SHINE data taking plan for 2017-18. The following abbreviations are used for the physics goals: SI – measurements for physics of strong interactions,  $\nu$  – measurements for the Fermilab neutrino beams.

Beam		Target	Momentum (A GeV/c)	Year	Days	Physics
Primary	Secondary					
P	h <sup>+</sup>	A	400 40-400	2017	21 days	installation/tests
P	p	Pb	400 30, 40	2017	28 days	SI
P	h <sup>+</sup>	A	400 30-120	2017	42 days	$\nu$
Xe		La	13, 19, 30, 40, 75, 150	2017	60 days	SI
P	p	Pb	400 13, 20	2018	28 days	SI
P	h <sup>+</sup>	A	400 30-120	2018	42 days	$\nu$
Pb		Pb	20, 40, 75, 150	2018	60 days	SI

## 6. Contributions of the JINR group and working plans for 2018-2020

According to the MoU the LHEP group of physicists from JINR is responsible for:

- **Maintenance of the TOF-L/R detector and its upgrade**
- **Software coordination and development:**  
(i.e. organization of the corresponding EVO meetings, assignment of different software tasks, migration of the NA61 software towards newer versions of compilers and operating systems, etc.)
- **Organization and maintenance of software releases;**
- **DAQ support and on-line data quality control during data taking:**  
(operation of the DAQ and on-line monitoring during the data-taking periods. The group has made a hardware contribution to the project of the on-line quality control: the corresponding PC is currently being used by the collaboration to build and view on-line histograms and to monitor the data quality);
- **Raw data processing for calibration and analysis:**  
(most of the NA61 data productions for calibration and analysis have been run by the members of the JINR group up to now. These data have been heavily used by the collaboration members and allowed for progress in calibration and detector understanding);
- **DST production:**  
(most of the existing DST productions for T2K and cosmic ray physics have been performed by physicists from the DLNP group and with their strong participation);
- **Data analysis**

Till the end of 2020 the VBLHEP team plans to obtain the following results:

- 1) participate in a full-scale NA61/SHINE physics run with the upgraded TOF scintillator detectors.
- 2) continue fulfilling responsibilities within the NA61/SHINE collaboration and assure simulation TOF software development.
- 3) perform analysis of light (anti)nuclei production in Xe+La collisions at 13-158A GeV.
- 4) continue R&D for MRPC TOF In particular:
  - integrate MRPC local readout electronics into the NA61 DAQ system;
  - make synchronization between the NA61 T0 and TOF systems;
  - evaluate the time resolution of the MRPC TOF system with T0 start;
  - match tracks from TPCs with MRPS hits;
  - make separation (identification) of hadrons;
  - develop and study new type of readout electronics with less than 3 ps time resolution to improve the identification ability of the MRPC TOF system.

The work-plan of the DLNP group of JINR physicists for 2018-2020 is following:

- 1) participation in the new period of data-taking at the CERN SPS;
- 2) fulfill responsibilities within the NA61/SHINE collaboration to assure software coordination and development as well as data processing for calibration and analysis.
- 3) Continue data analysis for the Fermilab neutrino program.

## 7. Required resources

In order to fulfill the above-mentioned tasks our estimation of the needed resources is shown in Table 5

Table 5. VBLHEP group resources for realization project in 2018-2020.

№	Expenditure	Full cost ( k\$ )	2018	2019	2020
	The direct costs of the project:				
1.	Nuclotron	-	-	-	-
3.	Computer communications	15	5	5	5
4.	Design Department	-	-	-	-
5.	LHEP workshops	-	-	-	-
6.	Materials	30	12	12	6
7.	Equipment	20	8	8	4
9.	Manpower at CERN	210	75	60	75
10	Collaboration common fund	36	12	12	12
	Total:	311	112	97	102

## References

- [1] C. Alt et al. [The NA49 Collaboration], Phys. Rev. C 77, 024903 (2007)
- [2] J. Bartke et al. [NA49-future Collaboration], A new experimental programme with nuclei and proton beams at the CERN SPS, CERN-SPSC-2003-038(SPSC-EOI-01)
- [3] N. Antoniou et al. [NA49-future Collaboration], Study of hadron production in collisions of protons and nuclei at the CERN SPS, CERN-SPSC-2006-001, CERN-SPSC-I-235.
- [4] N. Antoniou et al. [NA61 Collaboration], “Additional Information Requested in the Proposal Review Process (addendum to the proposal P330)”, CERN-SPSC-2007-004.
- [5] N. Abgrall et al. [NA61 Collaboration], CERN-SPSC-2007-033.
- [6] N. Abgrall et al. [NA61 Collaboration], “Proposal for secondary ion beams and update of data taking schedule for 2009-2013”, CERN-SPSC-2009-001.
- [7] N. Abgrall et al. [NA61 Collaboration], CERN-SPSC-2007-033, CERN-SPSC-P-330.
- [8] N. Abgrall et al. [NA61 Collaboration], CERN-OPEN-2008-012; CERN-Annual-Report-2007.
- [9] S. Afanasev et al. [NA49 Collaboration], Nucl. Instrum. Meth. A 430, 210 (1999).
- [10] J. Dainton et al., [The CERN SPS Committee], CERN-SPSC-2005-010, SPSC-M-730 (2005).
- [11] T. Akesson et al., “Towards the European strategy for particle physics: The briefing book,” arXiv:hep-ph/0609216.
- [12] Z. Fodor and S. D. Katz, JHEP 0404, 050 (2004)
- [13] C. R. Allton et al., Phys. Rev. D 71, 054508 (2005).
- [14] M. A. Stephanov, K. Rajagopal and E. V. Shuryak, Phys. Rev. D 60, 114028 (1999).
- [15] C. Alt et al. [NA49 Collaboration], Phys. Rev. Lett. 94, 052301 (2005).
- [16] M. A. Stephanov, Phys. Rev. D 65, 096008 (2002).
- [17] S. A. Bass et al., Prog. Part. Nucl. Phys. 41, 225 (1998).
- [18] C. Alt et al. [NA49 Collaboration], Nucl. Phys. A 774, 473 (2006).
- [19] P. Senger, T. Galatyuk, D. Kresan, A. Kiseleva and E. Kryshen, PoS C POD2006 (2006) 018.
- [20] G. S. F. Stephans, J. Phys. G 32 (2006) S447.
- [21] A. N. Sissakian, A. S. Sorin and V. D. Toneev, arXiv:nucl-th/0608032.
- [22] N. Abgrall et al., (NA61/SHINE Collab.) EPJ **C76** no. 2, (2016) 84.

- [23] A. Aduszkiewicz et al., (NA61/SHINE Collab.) Eur. Phys. J. **C76** no. 4, (2016) 198.
- [24] N. Abgrall et al., (NA61/SHINE Collab.) Eur. Phys. J **C76**, 617 (2016).
- [25] A. Aduszkiewicz et al., (NA61/SHINE Collab.) Eur. Phys. J. **C76**, 635 (2016).
- [26] T. Anticic et al. (NA49 Collaboration), Phys. Rev. C94, 044906 (2016).
- [27] T. Anticic et al. (NA49 Collaboration), Phys. Rev. C 85,044913 (2012).
- [28] T. A. Armstrong et al. (E864 Collaboration), Phys. Rev. C 61, 064908 (2000).
- [29] A. Andronic, P. Braun-Munzinger, and J. Stachel, Phys. Lett. B 673, 142 (2009).
- [30] J. Cleymans, H. Oeschler, K. Redlich, and S. Wheaton, Phys. Rev. C 73, 034905 (2006).
- [31] F. Becattini, M. Gazdzicki, A. Keranen, J. Manninen, and R. Stock, Phys. Rev. C 69, 024905 (2004).
- [32] V. Vovchenko, V. V. Begun, and M. I. Gorenstein, arXiv:nucl-th/1512.08025v1.
- [33] P. J. Siemens and J. I. Kapusta, Phys. Rev. Lett. 43, 1486 (1979).
- [34] V. Babkin, et al., Nucl. Inst. Meth. **A824** (2016) 490.
- [35] M.G. Buryakov et al., Phys.Part.Nucl.Lett. **13** No 5 (2016) 532.
- [36] <http://afi.jinr.ru/TDC72VHL>
- [37] V. Babkin, et al., Bulgarian Chemical Communications, **47**, Special Issue B (2015) 215.